

MCE-based Direct FTC Method for Dynamic Positioning of Underwater Vehicles with Thruster Redundancy*

Ji-Hong Li¹

Abstract—This paper presents an active model-based FTC (fault-tolerant control) method for the dynamic positioning of a class of underwater vehicles with thruster redundancy. Compared to the widely used state and parameter estimation methods, this proposed scheme directly utilizes the vehicle's motion control error (MCE) to construct a residual for detecting thruster faults and failures in the steady state of the control system. In the case of thruster fault identification, the most difficult aspect is that the actual control input with thruster faults is unknown. However, through a detailed and precise analyses of MCE variation trends in the case of thruster faults, highly useful information about this unknown control input can be extracted. This characteristic also serves as the foundation for the novel scheme proposed in this paper. As for control reconfiguration, it is straightforward since the thrust losses can be directly estimated as a result of the identification process. Numerical studies with the real world vehicle model are also carried out to demonstrate the effectiveness of the proposed method.

I. INTRODUCTION

Over the past few decades, interest in deep sea exploration has steadily grown, driven by its wide range of applications, including scientific research, resource exploration, oil and gas drilling, rescue operation, and various military activities. This insistent interest has fueled rapid advancements in underwater vehicle technology, further intensifying human curiosity about the deep sea.

Traditional ocean exploration typically consists of two consecutive steps of operations. The first one is a large-area survey conducted using torpedo-type autonomous underwater vehicles (AUVs), which are equipped with various sonar devices to inspect the seafloor environment. Once the AUV is recovered, recorded sonar images are manually analyzed to identify specific points of interest. The process then moves to the second step, where remotely operated vehicles (ROVs) or manned submersibles are deployed to these identified locations for detailed exploration and manipulation tasks, ultimately fulfilling the mission.

To ensure the reliability and safety of these expensive underwater robotic systems, ROVs and manned submersibles are typically designed with redundant thruster configurations. From a system science perspective, one of the most critical failure modes for these vehicles is thruster malfunction, alongside communication loss. As a result, the design of

fault-tolerant control (FTC) strategies to address thruster faults has emerged as a highly attractive research topic in robotics and control engineering.

This paper focuses on the model-based active FTC problem for a class of underwater vehicles with thruster redundancy. Compared to the related previous works, the main contributions of this work can be summarized as follows:

- The primary goal of thruster FTC is to ensure proper vehicle motion control. With this in mind, in this paper, motion control error (MCE) is directly applied to construct a residual for detecting fault and failure. This approach is significantly more compact compared to the previous works, which rely on estimation errors to generate residuals and therefore require an additional estimation scheme.
- A major challenge in thruster fault identification is the lack of knowledge about the actual control input when a fault occurs. However, through a detailed analysis of MCE variations under thruster faults, we demonstrate that valuable information about this unknown control input can be inferred—or even estimated. This insight plays a crucial role in the proposed fault identification scheme.
- Once thruster faults are identified through the proposed method, control reconfiguration or allocation becomes straightforward, as these corresponding thrust losses can be directly estimated as part of the identification process.

II. RELATED WORKS

Fault detection and identification (FDI) methods based on analytical redundancy have been widely studied in various complex dynamics systems [1], [2]. For some of large scale systems where dynamic modeling is prohibitively time-consuming, model-free method, especially using the expert system and artificial neural network, is suitable for their FTC [2], [3]. However, this method usually requires a suitable training set data, which is difficult to be acquired for many real-world dynamics systems. In addition, training neural networks, whether in off-line [4] or on-line [5] learning cases, can be computationally intensive and time-consuming [2]. In contrast, model-based method leverages the idea of generating residuals that reflect the inconsistency between actual and estimated behavior [2], [6]. State-estimation and parameter-estimation methods are two of most common schemes in this group [7]–[9]. These methods apply various system identification techniques to estimate system states or model parameters and using corresponding estimation errors

*This work was partially supported by the Korea Institute of Marine Science & Technology Promotion (KIMST) funded by the Ministry of Ocean and Fisheries (RS-2024-00432366), also in part by the same organization with the grant No. RS-2023-00256122, all in the Republic of Korea.

¹Ji-Hong Li is with the Autonomous Systems R&D Division, Korea Institute of Robotics and Technology Convergence, Jigok-Ro 39, Nam-Gu, Pohang 37666, Republic of Korea jhli5@kiri.ri.ac.kr

to construct proper residuals to detect and diagnosis the faults and failures.

This paper addresses the model-based active FTC problem for a class of underwater vehicles with thruster redundancy. Quite a number of related works have been done thus far [10]–[15]. In [11], state estimation error with all states measurable is used to detect the fault, and further an unknown input-observer is proposed to isolate this fault. In [12]–[14], a sliding-mode observer is used to estimate unmeasurable states and use the deviation of sliding surface of this observer in the steady state to detect and isolate the thruster fault and failure. For control allocation or reconfiguration, all the weight parameters for each thruster are adjusted iteratively until the residual minimization is ensured.

For most of practical underwater vehicles, especially expensive work-class ROVs and manned submersibles, a precise and reliable navigation system is the cornerstone of the entire vehicle system. These vehicles are usually equipped with various navigation systems (see [16] and references therein) combining with precious acoustic positioning system and navigation sensors, such as IMU (inertial measurement unit) and DVL (Doppler velocity log). Therefore, from a control engineering perspective, there is no need for additional observers to estimate the vehicle’s states. On the other hand, in the case of redundant system, it’s convenient to design a proper control method to guarantee the various performances in practice [17], [18]. Building on these two perspectives, in the authors’ previous work [19], a novel scheme of thruster FTC for a class of underwater vehicles with thruster redundancy is proposed. Instead of relying on estimation errors, the scheme directly utilizes the vehicle’s trajectory tracking error to construct a residual for detecting thruster faults and failures. For further fault identification, a novel diagnosis scheme is presented based on a detailed analysis of tracking error changing trends in response to variations in each thrust force in the steady state of control system. A key advantage of this approach is its ability to quickly and effectively pinpoint the faulty thruster by analyzing the trends of specific error combinations, such as 2D position and azimuth errors in the horizontal plane. As for control reconfiguration, the process is straightforward: the thrust loss parameter associated with the identified faulty thruster is adjusted until the residual falls below a specified threshold again.

This paper aims to extend the results from [19] to the case of dynamic positioning, with the following newly added contributions:

- Unlike [19], where no uncertainty term is considered in the vehicle’s dynamics, this paper accounts for unknown bounded uncertainty terms, including significant sea currents, for its dynamic positioning. All these uncertainties are assumed to be unmatched.
- In [19], the residual after the thruster fault remains elevated until the thrust loss parameter is adjusted to the correct value. In contrast, after the initial spike at the moment of thruster fault occurrence, the residual in this paper automatically decreases below the specified fault

detection criterion. For this reason, the method in [19] is not directly applicable to the case of dynamic positioning considered in this paper. However, this automatic decrease in residual also reveals an important property: the actual control input after thruster fault remains the same or very similar to the control input before the fault. Since this input matches the designed control input, it is known to us. Using this estimated actual control input after thruster fault, we can easily formulate the identification method and thrust loss estimation process. And this represents a key contribution of this paper.

- Furthermore, with this formulated identification method, the restrictive condition of *Assumption 3* in [19], which states that “at each time, only one thruster occurs fault or failure,” is removed in this paper. The proposed method in this paper can identify up to two simultaneous double thruster faults and can accurately estimate the thrust losses of each of them.

III. METHODOLOGY

A. Problem Statement

1) *Vehicle Model*: For most underwater vehicles, especially for work-class ROVs and manned submersibles, the center of gravity is often designed to be (much) lower than the center of buoyancy to stabilize roll motion. In addition, the thruster system is typically configured to allow easy decoupling of the vehicle’s horizontal and vertical motions, although vertical thrusters are sometimes used for tilt control. Considering these aspects and for the sake of discussion, this paper focuses solely on the vehicle’s 3DOF horizontal motion, with its kinematics and dynamics presented as follows [20].

$$\dot{\eta} = \mathbf{J}\boldsymbol{\nu}, \quad (1)$$

$$\mathbf{M}\dot{\boldsymbol{\nu}} + \mathbf{C}\boldsymbol{\nu} + \mathbf{D}\boldsymbol{\nu} + \mathbf{g}(\boldsymbol{\eta}) = \boldsymbol{\tau} + \mathbf{d}, \quad (2)$$

where $\boldsymbol{\eta} = [x, y, \psi]^T$ denotes the vehicle configuration on the horizontal plane in the navigation frame, and $\boldsymbol{\nu} = [u, v, r]^T$ is the velocity vector in the vehicle’s body-fixed frame, see Fig. 1; \mathbf{M} indicates the mass term including added mass, \mathbf{C} denotes the Coriolis and centripetal term, \mathbf{D} is the damping components, and \mathbf{g} presents gravitational term, all of which satisfy to be of class C^2 ; $\boldsymbol{\tau} = [\tau_u, \tau_v, \tau_r]^T$ is the thrust force and moment vector; \mathbf{d} denotes the uncertainty term including modeling errors, measurement noises, exogenous disturbances such as sea currents, etc., all of which are unmatched; \mathbf{J} denotes the coordinate transformation matrix from the vehicle’s body-fixed frame to the navigation frame, and can be expresses as follows,

$$\mathbf{J} = \begin{bmatrix} \cos \psi & -\sin \psi & 0 \\ \sin \psi & \cos \psi & 0 \\ 0 & 0 & 1 \end{bmatrix}.$$

For uncertainty term \mathbf{d} , we have the following assumption. *Assumption 1.* $|d_i| \leq D_{mi}$, $i = 1, 2, 3$ with $D_{mi} > 0$ unknown constant.

Considering (2), the vehicle’s dynamics usually satisfies the following properties [20], [21]

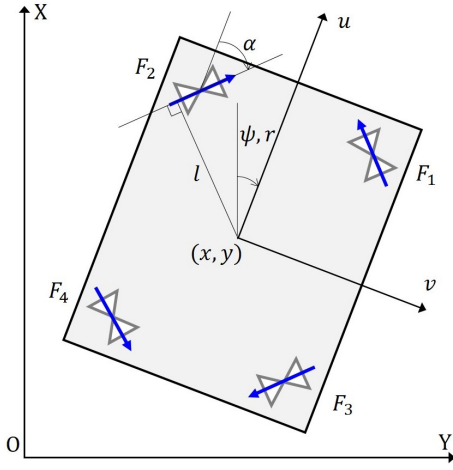


Fig. 1. Vehicle configuration in the navigation frame and its thruster configuration in the body-fixed frame.

P1. $M = M^T > 0$, and $\dot{M}(t) = 0$, $\forall t > 0$.

P2. $s^T [\dot{M} - 2C] s = 0$, $\forall s \in \mathfrak{R}^3$.

P3. $D > 0$.

Unlike previous related works [12]–[14], where the control laws are derived in the navigation frame, this paper directly solves the control problem in the vehicle's body-fixed frame as in (2).

For thruster configuration, we consider the case as shown in Fig. 1. This is also the most common configuration for underwater vehicles, where the arrangement of four horizontal thrusters has a symmetrical structure in the fore-aft and left-right directions. In this case, the control input $\tau = [\tau_u, \tau_v, \tau_r]^T$ can be presented as follows:

$$\begin{aligned} \tau &= \mathbf{T}_{conf} \mathbf{F} \\ &= \begin{bmatrix} \cos \alpha & \cos \alpha & -\cos \alpha & -\cos \alpha \\ -\sin \alpha & \sin \alpha & -\sin \alpha & \sin \alpha \\ -l & l & l & -l \end{bmatrix} \begin{bmatrix} F_1 \\ F_2 \\ F_3 \\ F_4 \end{bmatrix}, \end{aligned} \quad (3)$$

where α is the thruster orientation in the body-fixed frame and l denotes the distance from the center point to the thruster's orientation line.

2) Thruster Fault and Failure Model: For each thruster, its thrust output depends on the specific thruster model,

$$F_i = F_T(u_i), \quad (4)$$

where u_i is the thruster actual control input. Indeed, this is the input signal set into the thruster control board. In the case of BlueROV2 Heavy ROV [22], whose model will be used in the numerical studies in this paper, the thruster model (4) can be embodied as

$$F_i = K_i u_i, \quad (5)$$

with K_i the thrust coefficient. Here the sign of u_i indicates the thrust force direction: If $u_i > 0$, the thruster outputs forward thrust; otherwise, reverse thrust.

For thruster fault and failure model, this paper directly

implements the same model used in [10], [11] as follows:

$$F_i = K_i W_i u_i, \quad (6)$$

where W_i is a numerical weight indicating the thrust loss and defined as follows,

$$W_i = \begin{cases} 0 & \text{if } i\text{-th thruster has a failure} \\ 0 < W_i < 1 & \text{if } i\text{-th thruster is faulty} \\ 1 & \text{if } i\text{-th thruster is normal} \end{cases} \quad (7)$$

Consequently, the thruster force vector \mathbf{F} can be expressed as follows:

$$\mathbf{F} = \mathbf{K} \mathbf{W} \mathbf{u}, \quad (8)$$

where $\mathbf{K} = \text{diag}(K_1, \dots, K_4)$, $\mathbf{W} = \text{diag}(W_1, \dots, W_4)$, and $\mathbf{u} = [u_1, \dots, u_4]^T$.

Suppose τ_c is the control input calculated by the controller, then control allocation [23] is to allocate the actual control input \mathbf{u} as follows:

$$\mathbf{u} = \mathbf{W}^{-1} \mathbf{K}^{-1} \mathbf{T}_{conf}^\dagger \tau_c, \quad (9)$$

where superscript “ \dagger ” denotes the pseudo-inverse of a non-square matrix.

Here the problem is that, in practice, the exact value of \mathbf{W} is unknown, and therefore the control allocation has to take the following form

$$\hat{\mathbf{u}} = \hat{\mathbf{W}}^{-1} \mathbf{K}^{-1} \mathbf{T}_{conf}^\dagger \tau_c, \quad (10)$$

where $\hat{\mathbf{W}}$ is the estimation of \mathbf{W} and $\hat{\mathbf{u}}$ is the corresponding control allocation.

Consequently, the embodied control input τ becomes

$$\tau = \mathbf{T}_{conf} \mathbf{K} \mathbf{W} \hat{\mathbf{W}}^{-1} \mathbf{K}^{-1} \mathbf{T}_{conf}^\dagger \tau_c. \quad (11)$$

If $\hat{\mathbf{W}} = \mathbf{W}$, then we have $\tau = \tau_c$. Otherwise, the deviation of $\hat{\mathbf{W}}$ from \mathbf{W} can cause nonzero $\Delta\tau = \tau_c - \tau$, which further result in a similar deviation in the MCE during the steady state of the control system.

3) Problem Formulation: As in [19], this paper aims to answer the question, “*Is it possible to detect the change in \mathbf{W} and further identify which W_i is changed, by solely observing the deviation of MCE during the steady state of the control system?*”

To address this problem, this paper supposes the following constraint conditions.

Assumption 2. Thruster fault and failure occur only after the control system has been stabilized.

Assumption 3. Thruster fault and failure is caused only by the reduction of corresponding numerical scale weight \mathbf{W} .

Compared to [19], we can see that Assumption 3 in [19], which might be the most restricting condition in practical applications, is eliminated in this paper.

B. Motion Control Design

Let $\eta_d(t)$ denotes the vehicle's reference configuration and corresponding MCE is defined as $e_\eta(t) = \|\eta_d(t) - \eta(t)\|_2$. Here, if $\dot{\eta}_d = 0$, then this is regulation control problem, otherwise, becomes trajectory tracking problem. The control objective in this paper is to design a control law for τ so that

$e_\eta(t)$ to be uniformly ultimately bounded (UUB) with $t \rightarrow \infty$. For this purpose, the vehicle's kinematics and dynamics can be rewritten as follows:

$$\dot{e}_\eta = \eta_d - \mathbf{J}\nu, \quad (12)$$

$$\mathbf{M}\dot{\nu} = -\mathbf{C}\nu - \mathbf{D}\nu - \mathbf{g}(\eta) + \tau + \mathbf{d}. \quad (13)$$

For this second-order strict-feedback form of motion control system, general backstepping method [24] is utilized to solve the control problem.

1) *Step 1:* For given MCE $e_\eta(t)$, the following Lyapunov function candidate is considered in this step,

$$\mathbf{V}_1 = \frac{1}{2} \mathbf{e}_\eta^T \mathbf{\Gamma}_1 \mathbf{e}_\eta, \quad (14)$$

where $\mathbf{\Gamma}_1 > 0$ is a diagonal weighting matrix.

By differentiating (14) and substituting (13) into it, we get

$$\dot{\mathbf{V}}_1 = \mathbf{e}_\eta^T \mathbf{\Gamma}_1 (\dot{\eta}_d - \mathbf{J}\nu), \quad (15)$$

according to which, the following control law is chosen for α_ν , which is the stabilization function [24] for virtual control input ν in (15),

$$\alpha_\nu = \mathbf{J}^{-1} (\dot{\eta}_d + \mathbf{\Gamma}_1^{-1} \mathbf{A}_1 \mathbf{e}_\eta), \quad (16)$$

where $\mathbf{A}_1 > 0$ is diagonal control gain matrix.

By substituting (16) into (15), we have

$$\dot{\mathbf{V}}_1 = -\mathbf{e}_\eta^T \mathbf{A}_1 \mathbf{e}_\eta + \mathbf{e}_\eta^T \mathbf{\Gamma}_1 \mathbf{J} \mathbf{e}_\nu, \quad (17)$$

where $\mathbf{e}_\nu = \alpha_\nu - \nu = [e_u, e_v, e_r]^T$.

2) *Step 2:* Considering the vehicle's dynamics as (13) with properties P1–P3, the following Lyapunov function candidate is taken in this step.

$$\mathbf{V}_2 = \mathbf{V}_1 + \frac{1}{2} \left[\mathbf{e}_\nu^T \mathbf{M} \mathbf{e}_\nu + \tilde{\mathbf{D}}_m^T \mathbf{\Gamma}_2 \tilde{\mathbf{D}}_m \right], \quad (18)$$

where $\tilde{\mathbf{D}}_m = \hat{\mathbf{D}}_m - \mathbf{D}_m$ with $\mathbf{D}_m = [D_{m1}, D_{m2}, D_{m3}]^T$ and $\hat{\mathbf{D}}_m$ the estimation of \mathbf{D}_m , and $\mathbf{\Gamma}_2 > 0$ is a design diagonal weighting matrix.

By differentiating (18) and substituting (17) and (13) into it, we have

$$\begin{aligned} \dot{\mathbf{V}}_2 = & -\mathbf{e}_\eta^T \mathbf{A}_1 \mathbf{e}_\eta + \mathbf{e}_\eta^T \mathbf{\Gamma}_1 \mathbf{J} \mathbf{e}_\nu + \frac{1}{2} \mathbf{e}_\nu^T \dot{\mathbf{M}} \mathbf{e}_\nu \\ & + \mathbf{e}_\nu^T [\mathbf{M} \dot{\alpha}_\nu + (\mathbf{C} + \mathbf{D})\nu + \mathbf{g}(\nu) - \tau - \mathbf{d}] \\ & + \tilde{\mathbf{D}}_m^T \mathbf{\Gamma}_2 \dot{\tilde{\mathbf{D}}}_m. \end{aligned} \quad (19)$$

According to (19), we choose the control law for τ and corresponding adaptation law for $\hat{\mathbf{D}}_m$ as follows:

$$\tau = \mathbf{A}_2 \mathbf{e}_\nu + \mathbf{\Gamma}_1 \mathbf{J} \mathbf{e}_\eta + \mathbf{M} \dot{\alpha}_\nu + (\mathbf{C} + \mathbf{D})\alpha_\nu + \mathbf{g}(\eta) + \hat{\mathbf{d}}, \quad (20)$$

$$\dot{\hat{\mathbf{D}}}_m = \mathbf{\Gamma}_2^{-1} \mathbf{e}_\nu, \quad (21)$$

where $\mathbf{A}_2 > 0$ is diagonal control gain matrix, and $\hat{\mathbf{d}} \in \mathfrak{R}^3$ with $\hat{d}_i = \hat{D}_{mi} \varphi(\hat{D}_{mi} e_{\nu(i)})$. Here, the smooth function $\varphi(\cdot)$ satisfies the following lemma [25].

Lemma 1. $\forall \epsilon > 0$, there exist a smooth function $\varphi(\cdot)$ such that $\varphi(0) = 0$ and

$$|\xi| \leq \xi \varphi(\xi) + \epsilon, \quad \forall \xi \in \mathfrak{R}. \quad (22)$$

Remark 1. One example of smooth function satisfying Lemma 1 is $\varphi(\xi) = \tanh(\kappa \xi / \epsilon)$ with κ the solution of the equation $\kappa = e^{-(\kappa+1)}$ [25].

Theorem 1. Consider the trajectory tracking problem for (1) and (2). If we choose the control law as (20) and corresponding adaptation law as (21), then we can guarantee the closed-loop control system to be UUB.

Proof. By substituting (20) and (21) into (19), we can get

$$\begin{aligned} \dot{\mathbf{V}}_2 = & -\mathbf{e}_\eta^T \mathbf{A}_1 \mathbf{e}_\eta - \mathbf{e}_\nu^T \mathbf{A}_2 \mathbf{e}_\nu + \frac{1}{2} (\dot{\mathbf{M}} - 2\mathbf{C}) \mathbf{e}_\nu \\ & - \mathbf{e}_\nu^T \mathbf{D} \mathbf{e}_\nu - \mathbf{e}_\nu^T \mathbf{d} - \mathbf{e}_\nu^T \hat{\mathbf{d}} + \tilde{\mathbf{D}}_m^T \mathbf{e}_\nu \\ \leq & -\mathbf{e}_\eta^T \mathbf{A}_1 \mathbf{e}_\eta - \mathbf{e}_\nu^T \mathbf{A}_2 \mathbf{e}_\nu + \epsilon_1 + \epsilon_2 + \epsilon_3. \end{aligned} \quad (23)$$

In the final expansion, Lemma 1 is applied with $\epsilon_1, \epsilon_2, \epsilon_3 > 0$ the design parameters defined as in Lemma 1. (23) indicates that both of \mathbf{e}_η and \mathbf{e}_ν are all bounded by the constants $\epsilon_1, \epsilon_2, \epsilon_3 > 0$, and this concludes the proof. \square

Remark 2. Since $\epsilon_1, \epsilon_2, \epsilon_3 > 0$ can be chosen arbitrarily small, it's possible for us to get arbitrarily small value of MCE \mathbf{e}_η and \mathbf{e}_ν . However, too small value of ϵ_1, ϵ_2 , and ϵ_3 may cause certain high-gain control problem. Therefore, these parameters should be carefully chosen in practice.

C. Fault Detection and Identification

In practical applications, the thrusters are initially presumed to be functioning normally. In this case, we have $\hat{\mathbf{W}} = \mathbf{W} = \text{diag}(1, \dots, 1)$. Suppose there is a thrust loss $\Delta \mathbf{W}$ at $t = t_c > 0$. In this case, $\mathbf{W} = \hat{\mathbf{W}} - \Delta \mathbf{W}$, combining with which, (11) can be expanded as follows:

$$\begin{aligned} \tau &= \mathbf{T}_{conf} \mathbf{K} \mathbf{W} \hat{\mathbf{W}}^{-1} \mathbf{K}^{-1} \mathbf{T}_{conf}^+ \tau_c \\ &= \overbrace{\begin{bmatrix} \tau_1 & \tau_2 & \tau_3 & \tau_4 \\ -\tau_1 & \tau_2 & \tau_3 & -\tau_4 \\ -a\tau_1 & a\tau_2 & -a\tau_3 & a\tau_4 \end{bmatrix}}^{\mathbf{M}_\tau} \begin{bmatrix} 1 - \Delta W_1 / \hat{W}_1 \\ \vdots \\ 1 - \Delta W_4 / \hat{W}_4 \end{bmatrix} \\ &= \tau_c - \mathbf{M}_\tau \delta \mathbf{W}, \end{aligned} \quad (24)$$

where $\delta \mathbf{W} \in \mathfrak{R}^4$ with $\delta W(i) = \Delta W_i / \hat{W}_i$, $i = 1, \dots, 4$, and

$$\begin{bmatrix} \tau_1 \\ \tau_2 \\ \tau_3 \\ \tau_4 \end{bmatrix} = \begin{bmatrix} 1 & -1 & -1/a \\ 1 & 1 & 1/a \\ 1 & 1 & -1/a \\ 1 & -1 & 1/a \end{bmatrix} \tau_c = \mathbf{M}_c^T \tau_c, \quad (25)$$

with $a = l \sec \alpha = 0.267$. In the above expansion, for the sake of simplicity, we directly apply the parameters $\alpha = \pi/4$ and $l = 0.1888m$ of BlueROV2 Heavy ROV model [22].

Proposition 1. If the designed controller τ_c calculated as (20) has no component equal to zero, then \mathbf{M}_τ has rank 3.

Proof. Since \mathbf{M}_c has rank 3, τ_c with non component equal to zero can guarantee at least three of τ_i , $i = 1, \dots, 4$ are nonzero, which further guarantees \mathbf{M}_τ to be rank 3. \square

Remark 3. Here, it's worth to mention that all components of τ_c are nonzero is a sort of sufficient condition, not necessary one. It's easy to see that any of $\tau_c \in \{[\zeta, 0, 0]^T, [0, \zeta, 0]^T, [0, 0, \zeta]^T\}$ with $\zeta \neq 0$ can guarantee all

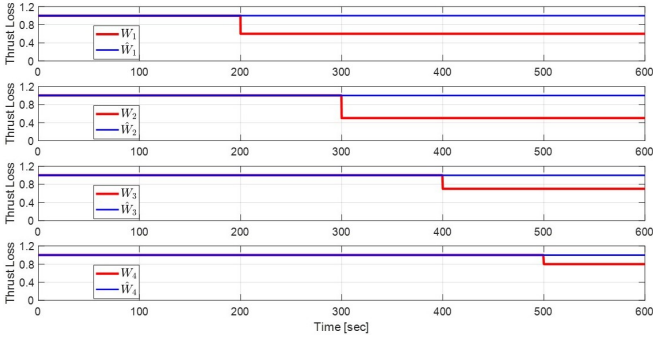


Fig. 2. Thruster fault occurrence scenario.

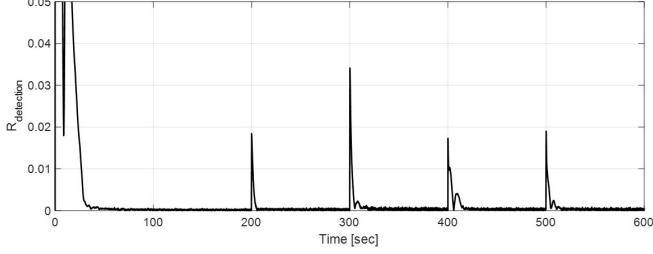


Fig. 3. Corresponding residual measurement.

τ_i to be nonzero, and therefore easy to guarantee the same result of M_τ having rank 3.

Remark 4. If M_τ has rank 3, it is straightforward to verify that up to two simultaneous thruster faults can be identified. However, in the case of three simultaneous thruster faults, it is, in principle, impossible to distinguish this fault from the one where the remaining single thruster occurs fault.

Remark 5. It is also worth noting that although no component of τ_c is exactly zero, it still possible for one of τ_i , $i = 1, \dots, 4$, to be equal or near zero. In this case, from (24), the corresponding column vector in M_τ becomes one with components of zero or very small magnitude. Consequently, the thrust loss associated with this column vector may not be sufficiently reflected in the residual, making it undetectable. To the best of the authors' knowledge, such detection failure is expected to be challenging regardless of any additional estimation methods applied.

If τ is known after $t > t_c$, then through (24), it's possible for us to identify δW . The problem is that, in practice, it's impossible to know τ since W is unknown after $t > t_c$. To solve this problem, we carry out a simulation study using BlueROV2 model [22] and investigate the similar case. In the simulation, the control law (20) is applied with the adaptation law taken as (21). Other detailed simulation conditions will be illustrated in Section IV.

Simulation results are shown in Fig. 2–4. Fig. 2 shows the sequential occurring of thruster faults, and corresponding residual changing trend is presented in Fig. 3, from which we can see that the constructed residual is suitable to detect the thruster faults. An additional point to note in Fig. 3 is that, after sparking at the time of ΔW occurrence, $R_{detection}$ automatically decreases again. This is a significantly different trend from the case in the authors' previous work [19], where

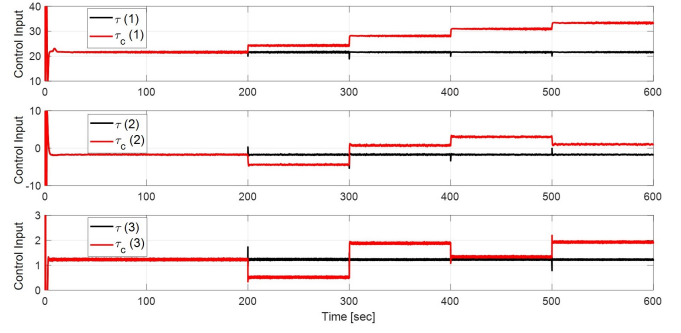


Fig. 4. Corresponding time variations of designed controller τ_c and actual control input τ .

the residual stays elevated if \hat{W} remains unchanged. To the authors' knowledge, this kind of auto-decreasing of residual is due to the adaptation component \hat{d} in the control law (20). Compared to the previous work [19], this kind of auto-decreasing of residual imposes two challenges; one is making it difficult to evaluate the magnitude of ΔW , and the other is that the criterion for adjusting \hat{W} disappears. So we need to explore a new criterion for fault identification that can replace the residual in [19]. Fortunately, from Fig. 4, we can see that: before thruster faults occurrence ($t < 200s$), τ_c is exactly the same as τ , and along with the sequential occurrences of thruster faults, compared to τ_c , which correspondingly changes over the faults, τ always maintains its original value as in $t < 200s$ (except for the sparking at the very moment of fault occurrences). This also coincides with the result in Fig. 3. To conclude, the actual control input τ after thruster faults occurrence can be approximated as τ_c in the steady state case before thruster fault. Therefore, (24) can be rewritten as

$$M_\tau \delta W = \tau_c |_{t>t_c} - \tau_c |_{t<t_c} + w, \quad (26)$$

where $w = \tau - \tau_c |_{t>t_c}$.

In this paper, w is assumed to be a zero mean random noise. Since M_τ and τ_c are always known, now we can identify the thruster faults δW .

1) *Fault Detection:* Residual $R_{detection}$ is defined as follows [19]:

$$R_{detection} = \sqrt{x_e^2 + y_e^2 + c_1 \psi_e^2}, \quad (27)$$

where $c_1 > 0$ is a normalization constant parameter. At each time $t > 0$, fault detection for the calculated residual $R_{detection}$ is simple and can be described as follows:

```

if ( $R_{detection} > c_2$ )&&(bFirst == 1)
    faultTrig = true;
    bFirst = 0;
end if

```

where $c_2 > 0$ is a constant criterion.

2) *Fault Identification:* Fault identification follows the detection phase with $faultTrig = true$, see Algorithm 1.

In Algorithm 1, τ_c represents both of $\tau_c |_{t<t_c}$ and $\tau_c |_{t>t_c}$; $c_3, c_4 > 0$ are criterion parameters; $T_3 > T_2 > T_1 > t_c$ are time-related parameters, where t_c represents the fault

Algorithm 1: Fault Identification ()

Input: M_τ, τ_c, \hat{W}

- 1 **waiting for** faultTrig=true
- 2 $dW_1 = 0; dW_2 = [0; 0]; nC = 0;$
- 3 **while** (faultTrig)
- 4 **if** ($t - t_c > T_1$)
- 5 $[\delta W_n, rmse, n] = tFaultID(M_\tau, \tau_c, \hat{W}, single)$
- 6 **if** $rmse \leq c_3$
- 7 $dW_{1+} = \delta W_n;$
- 8 $nC++;$
- 9 **if** $t - t_c == T_2$
- 10 $\hat{W}(n, n) = \hat{W}(n, n)(1 - dW_1/nC);$
- 11 **end if**
- 12 **else**
- 13 $[\delta W_{n_1}, \delta W_{n_2}, rmse, n_1, n_2] =$
 $tFaultID(M_\tau, \tau_c, \hat{W}, double)$
- 14 **if** $rmse \leq c_4$
- 15 $dW_{2+} = [\delta W_{n_1}; \delta W_{n_2}];$
- 16 $nC++;$
- 17 **if** $t - t_c == T_2$
- 18 $\hat{W}(n_1, n_1) = \hat{W}(n_1, n_1)(1 - dW_2[1]/nC);$
- 19 $\hat{W}(n_2, n_2) = \hat{W}(n_2, n_2)(1 - dW_2[2]/nC);$
- 20 **end if**
- 21 **end if**
- 22 **end if**
- 23 **end if**
- 24 **if** $t - t_c == T_3$
- 25 $faultTrig=false;$
- 26 $bFirst=1;$
- 27 **end if**
- 28 **end while**
- 29 **end waiting for**
- 30 **return**

occurrence time. At each $t = t_c$, the designed control input τ_c experiences magnitude jumps, and T_1 is used to allow for the convergence of this jumped $\tau_c(t)$. Due to the presence of random noise w as in (26), the estimated thrust loss δW_i also contains random noise. To mitigate this effect, T_2 is used to attenuate the impact of this noise by simply averaging the estimation δW_i over the period $T_2 - T_1$. Each occurrence of control allocation at $t = t_c + T_2$ using updated thrust loss parameter \hat{W} is typically followed by a spike in $R_{detection}$. To account for this, T_3 is applied to allow for the re-convergence of $R_{detection}$ after $t = t_c + T_2$.

To illustrate the core function $tFaultID()$ in Algorithm 1, we rewrite (26) as follows:

$$\begin{bmatrix} \tau_1 & \tau_2 & \tau_3 & \tau_4 \\ -\tau_1 & \tau_2 & \tau_3 & -\tau_4 \\ -a\tau_1 & a\tau_2 & -a\tau_3 & a\tau_4 \end{bmatrix} \begin{bmatrix} \delta W_1 \\ \vdots \\ \delta W_4 \end{bmatrix} = \mathbf{b}_\tau, \quad (28)$$

where $\mathbf{b}_\tau = \tau_c |_{t>t_c} - \tau_c |_{t<t_c}$.

From (28), we can see that in the case of single thruster fault, identification problem becomes to find out a vector among four column vectors of M_τ , which is parallel to \mathbf{b}_τ and points in the same direction as \mathbf{b}_τ . Corresponding pseudo code for this process is shown in Algorithm 2, where $rmse$

means root mean square error.

Algorithm 2: $tFaultID(M_\tau, \tau_c, \hat{W}, single)$

- 1 **for** $i=1:4$
- 2 $\delta W[i] = M_\tau^\dagger(:, i)\mathbf{b}_\tau;$
- 3 $rmse[i] = \sqrt{\frac{1}{3} \sum_{j=1}^3 [b_\tau(j) - \delta W[i]M_\tau(j, i)]^2};$
- 4 **end for**
- 5 **return** minimum $rmse[i]$ and corresponding $\delta W[i]$ and i

In the case of double thruster faults, the identification process is similar to that in Algorithm 2, except that the column vector in Algorithm 2 is replaced by a combination of two column vectors from M_τ . Given four column vectors $M_\tau(:, i)$, $i = 1, \dots, 4$, there are a total of six different combinations of two columns. Let Ω denotes a 3×2 matrix set consisting of these six different combinations. The identification process for double thruster faults can then be described as in Algorithm 3.

Algorithm 3: $tFaultID(M_\tau, \tau_c, \hat{W}, double)$

- 1 Construct Ω from $M_\tau;$
- 2 **for** $i=1:6$
- 3 $\mathbf{a}_i \in \Omega;$
- 4 $\delta W(:, i) = \mathbf{a}_i^\dagger(:, i)\mathbf{b}_\tau;$
- 5 $rmse[i] = \sqrt{\frac{1}{3} \sum_{j=1}^3 [b_\tau(j) - \delta W(1, i)\mathbf{a}_i(j, 1) - \delta W(2, i)\mathbf{a}_i(j, 2)]^2};$
- 6 **end for**
- 7 **return** minimum $rmse[i]$ and corresponding $\delta W(:, i)$ and i

In Algorithm 3, from returned case number i , we can further decode the corresponding column numbers $j, k \in \{1, \dots, 4\}$ with $\mathbf{a}_i = [M_\tau(:, j); M_\tau(:, k)]$.

3) *Control Allocation:* Control allocation can be efficiently achieved using (10), where \hat{W} is replaced with the estimated values as specified in Algorithm 1 (line 10 or line 18 and 19).

IV. NUMERICAL STUDIES

The 3DOF horizontal dynamic positioning of an underwater vehicle in a strong sea current environment is considered in this numerical studies. As mentioned before, the 6DOF nonlinear model of BlueROV2 Heavy ROV [22] is directly applied in the Matlab-based simulation. The sea current is simulated with $u_c = 1.0m/s$ and $\psi_c = -120^\circ$, while the remaining uncertainty terms are set as $\mathbf{d} - \mathbf{d}_{sc} = [1 - 2rand; 1 - 2rand; 0.03(1 - rand)]$ with \mathbf{d}_{sc} indicating the aforementioned sea current. Here, $rand \in [0, 1]$ denotes a random variable.

For the vehicle's thruster configuration, we have $\mathbf{K} = diag(40, 40, 40, 40)$, $\alpha = 45^\circ$ and $l = 0.1888m$. The vehicle's dynamic positioning reference configuration is set as $\boldsymbol{\eta}_d = [10m, 2m, 70^\circ]^T$, and the vehicle's initial state is chosen as $\mathbf{X}(0) = \mathbf{0}^{12 \times 1}$ (in the simulation, 6DOF model is used instead of 3DOF). Controller design parameters are set as $\Gamma_1 = diag(1, 1, 1500)$, $\Gamma_2 = diag(1, 1, 0.6)$,

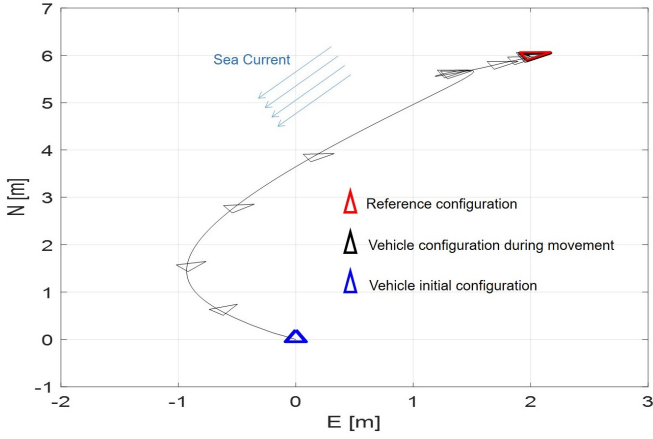


Fig. 5. Vehicle trajectory during the dynamic positioning without thrust loss parameter update.

$\mathbf{A}_1 = \text{diag}(1.5, 1.5, 5)$, $\mathbf{A}_2 = \text{diag}(1, 1, 12)$, $\hat{\mathbf{D}}_m = \mathbf{0}^{3 \times 1}$, and $\epsilon_1 = \epsilon_2 = \epsilon_3 = 0.1$. For the smooth function $\varphi(\cdot)$, it is chosen as $\varphi(\xi) = \tanh(\kappa\xi/\epsilon)$ in the simulation with $\kappa = 0.2785$ [25]. FDI algorithm related parameters are chosen as: $c_1 = (180/\pi)^2$, $c_2 = 0.005$, $c_3 = c_4 = 0.1$, $T_1 = 20s$, $T_2 = 25s$, and $T_3 = 35s$. Finally, the algorithm sampling time is set as $0.01s$.

In the simulation, we carry out various case studies, among which Fig. 2–4 present a scenario where sequential thruster faults occur as $W_1 \rightarrow W_4$, without control allocation based on thrust loss parameters estimation (line 10 in Algorithm 1 is not executed). Fig. 5 shows the vehicle's trajectory for this case study, which closely resembles the trajectory observed when no thruster fault occurred. Some interesting results from other case studies are summarized below.

1) *A Single Thruster Fault with Sequential Thrust Loss Leading to Failure*: The simulation results for this case are presented in Fig. 6 and 7. Fig. 6 demonstrates that the proposed FDI algorithm effectively detects and identifies faults while maintaining accurate estimation capability. Notably, as shown in Fig. 7, following the single thruster failure at $t_c = 1000s$, the residual exhibits a slight increase compared to the previous sequential stages, highlighted by the red-dotted circle. This suggests a discontinuity in control allocation at the moment when the thruster configuration transitions from four thrusters to three.

2) *Combination of Single and Double Thruster Faults*: The corresponding case study results are shown in Fig. 8, demonstrating that the proposed scheme effectively detects and identifies both single and double thruster faults while maintaining accurate estimation performance. In fact, we carried out a large number of similar case studies and observed consistent results throughout.

3) *Fault Detection Failure*: If we set $\boldsymbol{\eta}_d = [10, 2, 90^\circ]^T$ instead of $\boldsymbol{\eta}_d = [10, 2, 70^\circ]^T$, then \mathbf{M}_τ takes the following form:

$$\mathbf{M}_\tau = \begin{bmatrix} 3.5178 & 5.0833 & -0.7511 & 9.3522 \\ -3.5178 & 5.0833 & -0.7511 & -9.3522 \\ -0.9393 & 1.3572 & 0.2006 & 2.4971 \end{bmatrix}, \quad (29)$$

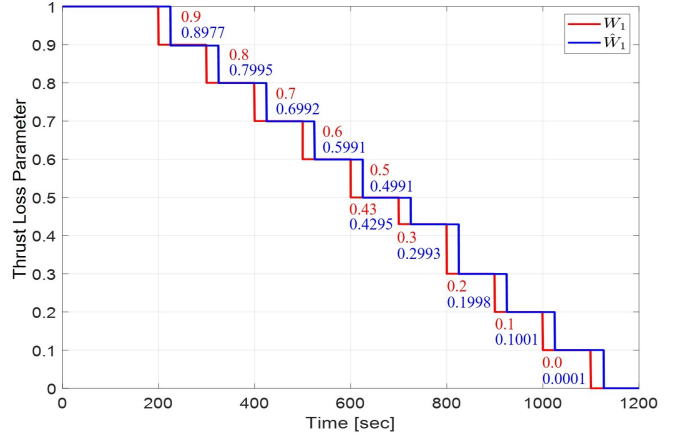


Fig. 6. Single thruster sequential faults and their detection, identification, and corresponding thrust loss estimations.

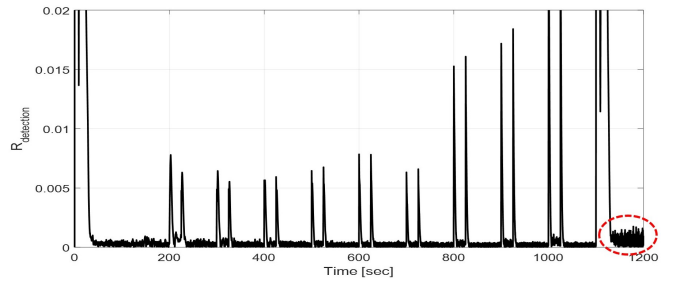


Fig. 7. Residual variation trend during sequential single thruster faults leading to failure.

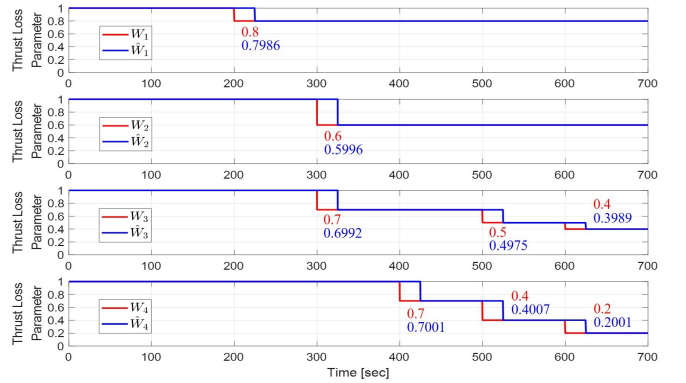


Fig. 8. Detection, identification, and thrust loss estimation for single and double thruster fault combinations.

where the third column has relatively small component magnitude compared to the others. In this case, if we set $\delta W_3 = 0.1$, indicating a relatively small thrust loss for the third thruster, Fig. 9 shows that the proposed FDI algorithm fails to detect this fault, which further causes the detection failure of W_4 at $t = 500s$. However, when the thrust loss is increased to $\delta W_3 = 0.3$, both δW_3 and δW_4 becomes detectable, see Fig. 10. As mentioned in Remark 5, in the specific case of τ_c which causes one of τ_i , $i = 1, \dots, 4$ to be equal or near zero, the thrust loss in this i th thruster becomes difficult to be detected. This could be recognized as an inherent limitation of the FDI algorithm proposed in

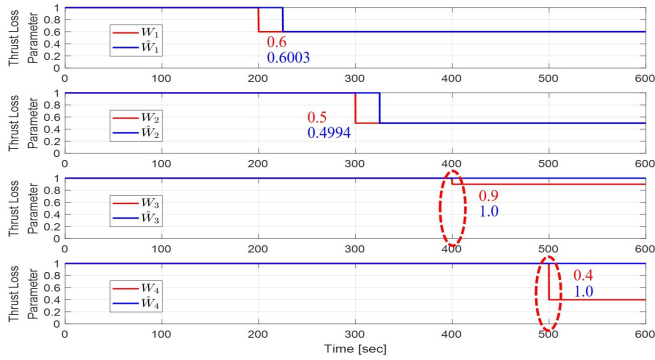


Fig. 9. Failure of fault detection in the case of a small thrust loss in the thruster, which corresponds to the third column vector of M_T in (29), having small magnitude components.

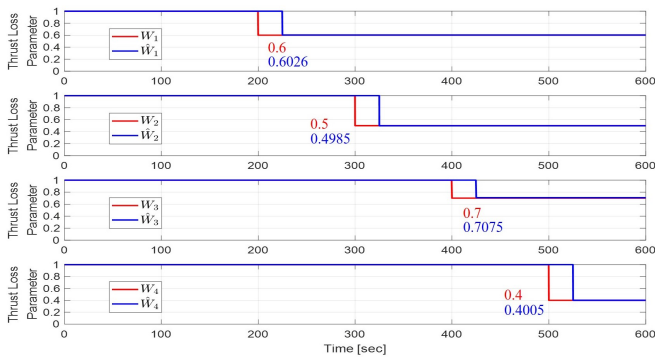


Fig. 10. Successful fault detection with increasing thrust loss in the third thruster, while maintaining the same conditions as in Fig. 9.

this paper.

V. CONCLUSION

This paper has presented a novel FTC scheme for a class of underwater vehicles with thruster redundancy. Rather than relying on estimation errors, the residual is constructed by directly applying MCE, eliminating the need for an additional estimation system. Through detailed and precise analyses of MCE variation trends in the presence of thruster faults, valuable information regarding the actual control input after a thruster faults can be acquired, allowing us to formulate both the fault identification method and the thrust loss estimations. The proposed FDI algorithm can handle up to two simultaneous thruster faults. Various numerical studies have been carried out, demonstrating that the proposed method provides satisfactory FDI performance and accurate thrust loss estimation.

Since the thruster configuration matrix is 3×4 , in principle, simultaneous faults in three thrusters cannot be distinguished from a fault in the remaining single thruster. However, by restricting each thrust loss to the domain $[0, 1]$, it may be possible to solve this triple-fault problem. Therefore, this will be an interesting topic for our future research.

REFERENCES

[1] R. J. Patton, R. M. Frank, R. N. Clarke. *Fault Diagnosis in Dynamic Systems: Theory and Application*. Prentice-Hall, Inc., 1989.

[2] L. Ni. *Fault-Tolerant Control of Unmanned Underwater Vehicles*. Ph.D. Thesis, Department of Mechanical Engineering, Virginia Polytechnic Institute and State University, 2001.

[3] R. F. Stengel, "Intelligent Failure-Tolerant Control," in *Proc. of 5th IEEE International Symposium on Intelligent Control*, Philadelphia, PA, 1990, pp. 548–557.

[4] S. Naidu, E. Zafiriou, T. McAvoy, "Use of Neural Networks for Sensor Failure Detection in a Control System," *IEEE Control System Magazine*, vol. 10, pp. 49–55, 1990.

[5] D. J. Linse and R. F. Stengel, "A System Identification Model for Adaptive Nonlinear Control," in *Proc. of American Control Conference*, Boston, MA, 1991, pp. 1752–1757.

[6] J. Gertler, "Survey of Model-Based Failure Detection and Isolation in Complex Plants," *IEEE Control System Magazine*, vol. 10, pp. 18–23, 1990.

[7] P. M. Frank, "Fault Diagnosis in Dynamic System Using Analytical and Knowledge-Based Redundancy – A Survey and Some New Results," *Automatica*, vol. 26, No. 3, pp. 459–474, 1990.

[8] T. E. Menke and P. S. Maybeck, "Sensor/Actuator Failure Detection in the Vista F-16 by Multiple Model Adaptive Estimation," *IEEE Transactions on Aerospace & Electronic Systems*, vol. 31, no. 4, pp. 1218–1228, 1995.

[9] R. Isermann, "Process Fault Detection Based on Modeling and Estimation Methods – A Survey," *Automatica*, vol. 20, no. 4, pp. 387–404, 1984.

[10] J. Jiang and X. Yu, "Fault-Tolerant Control Systems: A Comparative Study Between Active and Passive Approaches," *Annual Reviews in Control*, vol. 36, no. 1, pp. 60–72, 2012.

[11] A. Cristofaro and T. A. Johansen, "Fault Tolerant Control Allocation Using Unknown Input Observers," *Automatica*, Vol. 50, pp. 1891–1897, 2014.

[12] M. L. Corradini and G. Orlando, "A Robust Observer-Based Fault Tolerant Control Scheme for Underwater Vehicles," *Journal of Dynamic Systems, Measurement, and Control*, vol. 136, no. 3, 2014, <https://doi.org/10.1115/1.4026328>.

[13] M. L. Corradini and A. Cristofaro, "A Nonlinear Fault-Tolerant Thruster Allocation Architecture for Underwater Remotely Operated Vehicles," *IFAC-PapersOnLine*, 49–23, 2016, pp. 285–290.

[14] A. Baldini, A. Fasano, R. Felicetti, A. Freddi, S. Longhi, A. Monteriu, "A Model-based Active Fault Tolerant Control Scheme for a Remotely Operated Vehicle," *IFAC PapersOnLine*, 51–24, 2018, pp. 798–805.

[15] F. Liu, Z. Ma, B. Mu, C. Duan, R. Chen, Y. Qin, H. Pu, J. Luo, "Review on Fault-Tolerant Control of Unmanned Underwater Vehicles," *Ocean Engineering*, vol. 285, 115471, 2023.

[16] J. H. Li, M. G. Kim, H. Kang, M. J. Lee, G. R. Cho, S. Kang, "Initial Alignment and Position Aiding Time Delay Compensation for SDINS of Deep Sea Underwater Vehicle," in *Proc. of American Control Conference*, Atlanta, GA, 2022, pp. 3126–3131.

[17] J. Yuh, T. Ura, G. A. Bekey. *Underwater Robots*. Kluwer Academic Publishers, 1996.

[18] J. H. Li and P. M. Lee, "Neural Network Adaptive Control for a Class of Nonlinear Systems with Unknown-Bound Unstructured Uncertainties," in *Proc. of 43rd IEEE Conference on Decision and Control*, Atlantis, Bahamas, 2004, pp. 692–697.

[19] J. H. Li, H. Kang, M. G. Kim, M. J. Lee, H. S. Jin, G. R. Cho, "Tracking Error Based Fault Tolerant Scheme for Marine Vehicles with Thruster Redundancy," arXiv preprint arXiv:2501.18852, <https://doi.org/10.48550/arXiv.2501.18852>, 2025.

[20] T. I. Fossen. *Handbook of Marine Craft Hydrodynamics and Motion Control*. John Wiley & Sons, 2011.

[21] J. H. Li, H. Kang, M. G. Kim, M. J. Lee, H. S. Jin, G. R. Cho, "A Lagrangian Approach for Trajectory Tracking of Underactuated Marine Vessels," *IFAC PapersOnLine*, vol. 58, no. 6, pp. 196–201, 2024.

[22] C. J. Wu. *6-DOF Modelling and Control of a Remotely Operated Vehicle*. B.Eng. Thesis, Engineering Discipline College of Science and Engineering, Flinders University, 2018.

[23] T. A. Johansen and T. I. Fossen, "Control Allocation—A survey," *Automatica*, vol. 49, pp. 1087–1103, 2013.

[24] M. Krstic, I. Kanellakopoulos, P. Kokotovic. *Nonlinear and Adaptive Control Design*. John Wiley & Sons, Inc., New York, 1995.

[25] J. H. Li, "Path Tracking of Underactuated Ships with General Form of Dynamics," *International Journal of Control*, vol. 89, pp. 506–517, 2016.